Chapter 3

FACILE POLYMER MACROLENS FABRICATION FOR ENHANCED MAGNIFICATION PHOTOMICROGRAPHY

3.1 CHAPTER OUTLINE

Observing micron size objects and image capturing using low-cost cellphone-based microscopy, is of immense potential in biomedical instrumentation and diagnosis. In recent times when facile methods of microfabrication are under development, a handy method to observe micron-size features is much needed. The present study aims to fabricate millimeter-size lens attachments using simple thermal processing, which enables a general user to observe micrometer-size features using a cellphone camera (8 MP and (1/f)=0.21). These lenses are easy to fabricate, stable, and demonstrated to be almost free from chromatic aberration. In this chapter, we aim to understand the polymer behavior near glass transition temperature and free volume adjustment without compromising its transparency. Self-organized structures obtained after thermal melting was used as a lens attachment to the cellphone camera. This lens attachment shows the efficiency of the lens-cellphone camera combination, which gives 5-10 times additional magnification with significant clarity, compared to the cellphone camera alone. Potential uses of this set-up can be observing bacteria colonies, the prognosis of Skin fungal infection, wastewater treatment, etc. This technology in combination with Image processing tools can open up an immense potential scope in biomedical Imaging and lab on chip-based optical devices.

3.2 INTRODUCTION

Low-cost microscopy is the need of the hour for efficient healthcare service delivery and wastewater assessment.[1,2] High cost and training associated with sophisticated imaging instruments have hindered the wide reach of healthcare facilities in developing countries.[3] Since cellphone subscriptions worldwide are ubiquitous, a possible solution will be the use of cellphone-based low-cost microscopy, which has been the focus of many research groups.[4-6] Cellphone-based microscopy has been demonstrated to be useful in malaria parasite testing[7], sperm tracking[8-10], wastewater quality assessment[11,] etc. Based on optical setup cellphone-based microscopy can be categorized into three parts (a) on-chip analysis (b) off chip clip on arrangement (c) On lens arrangement.

On-chip analysis is mainly holographic imaging, where an additional sensor or detector array is used to capture diffraction patterns and fringe patterns, and reconstruction of the image is done.[12,13] This method does not require an additional lens, hence there is no limit to the numerical aperture, and thus better light collection efficiency and increased resolution are achieved. However these methods require intrusive modification in the cellphone camera hardware, and generally, an additional image processing tool and an original standard photograph for the reconstruction of the image are required. Off-chip analysis, on the other hand, is comprised of several clip-on arrangements to increase magnification and resolution.[14] A setup consisting of a microscope objective interfaced to a cellphone camera using a lens tube and eyepiece has been studied for increased magnification.[4] A 3D printed chassis and stage setup have been developed to devise a miniaturized benchtop microscope.[15] Such arrangements are easy to use but their applications are limited as the setup is bulky and customized for individual

cellphone models. Thus a clip-on arrangement usually works with a dedicated cellphone model and the viewpoint of the specimen is also restricted.

The third approach of cellphone microscopy is on lens approach, where an external refractive lens attachment is placed in front of the integrated cellphone camera lens.[16-18] Along with an external light source, it can form a transmission mode bright field microscope with enough magnification to image red blood cells and platelets.[19] Such arrangements are robust and can be used by an ordinary user. There have been several attempts to achieve better magnification and resolution using lens attachment-based low-cost microscopes. However, there is a significant scarcity of rapid effective, and facile methods of fabrication for such lens attachments. A cheap and easy fabrication method of such lens attachments is required which can be very useful in healthcare, education, and wastewater assessment in a remote setup.

Fabrication of PDMS lenses for cellphone camera attachment has been studied earlier.[20-22] However, the method of fabrication, control over shape & size, and getting a sharp focal spot for imaging has always been a laborious task. Aspherical lenses developed by Roy et al. have been demonstrated to focus light. However, these optofluidic lenses are made up of PDMS filled with liquid, they can be easily distorted by mechanical stress. Due to lower surface energy, it attracts dust particles, and the durability of such lenses in an open environment is limited. These lenses are more useful as waveguides, however, imaging through such lenses have found to be very difficult. Though these lenses can be tuned in real-time, it requires additional setup, and cannot be used for a point-of-care optical imaging system. In this chapter, we have fabricated polystyrene lenses, to image the microparticles in combination with a cellphone camera. We want to substitute the use of the standard microscope in the previous chapter, with a cellphone and macro lens attachment. Fabrication of lenses, with quite good control over

shape and size by controlling temperature, molecular weight, and weight of the polystyrene is presented. The dependence of different parameters such as numerical aperture and focal length on the weight of the polymer is established. The lensing effect of such lenses is also demonstrated to have 5-10 times add-on magnification without any post-capture image processing, which can be very useful in different healthcare and waste water quality assessment applications.

3.3 EXPERIMENTAL METHODOLOGY

A simple thermal melting and self-organization of polymer pellets of different molecular weights and masses were used to shape opaque pellets into transparent lenses. Molecular rearrangement to reduce the free volume of the polymer and obtain a semispherical shape due to surface tension made the formation of lenses self-organizing. Comparison with commercially available lenses using simulation tools and magnification/resolution results were demonstrated.

3.3.1 Material Selection and Lens Fabrication

The most important aspect of lens fabrication is the material selection. Materials used for lens fabrication are primarily polymeric materials. Low cost, easy thermal processing compared to glass, self-assembling and high optical transmittance of polymers offer easy tailoring of optical structures. Therefore, we have selected polystyrene which has a higher refractive index (n =1.59), is thermally stable up to 100°C (T_g >100°C), and is resistant to most of the aqueous solutions. By far the most commonly used materials for optical elements are glass and quartz, which have lower refractive index than polystyrene. The processing advantage of polystyrene over glass and quartz facilitates low-cost lens fabrication.

Polystyrene of two different molecular weights 192K gram/mole and 280K gram/mole represented as polymers 1 and 2 hereafter, were melted at four different temperatures ranging from 120°C to 240°C for three hours. The weight of the polymer pellets varied to achieve different shapes and sizes. Physical measurement of numerical aperture and focal length is done and a relation of these parameters with the weight of the polystyrene is established. Feature comparison of the focus spot diagram and Optical Path Difference (OPD) diagram of the fabricated lens and the commercially available lens is presented using the Zemax OpticSudio simulation platform. Practically magnification of lenses was observed using reflection mode imaging of a 435PPI pixel pattern of cellphone display and observation of onion peel.

3.3.2 Magnification and Resolution Analysis

The Lenses were tested using two ways 1) when kept near the object and 2) when kept near the camera. An additional test using a microscope was done if it enhances the performance of the microscope. Onion peel was observed using a microscope with and without focusing through lenses. A schematic diagram of schemes 1 and 2 mentioned above is shown in Figure 3.1.

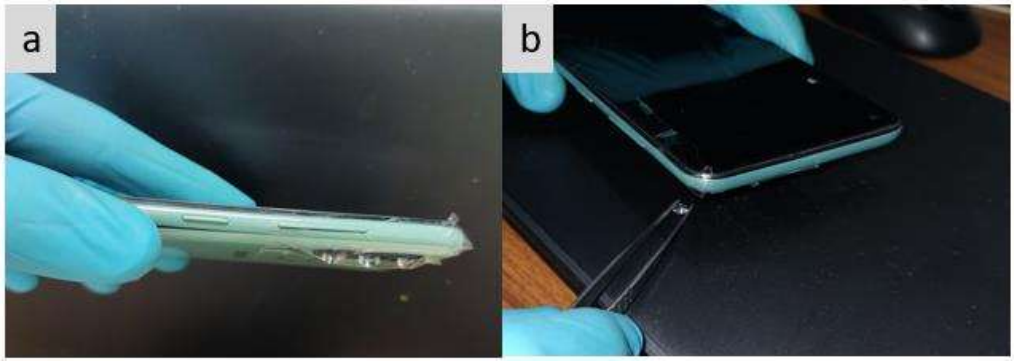

Figure 3.1 Two different schemes of imaging of lens and cellphone camera combination a) when lens is attached to the camera, b) when lens is near object.

3.4 RESULT AND DISCUSSION

Firstly, the quality of lenses and their theoretical understanding were developed. Chromatic aberration and the focal spot were discussed using the simulational tool. Further magnification and resolution of the lenses were discussed.

3.4.1 Polystyrene Lens Fabrication

Heating the polystyrene over its glass transition temperature allows the polymer to reflow, and the surface tension dictates the spherical shape of the polymer pellet. Polystyrene pellets of two different molecular weight and the same weight is heated in a temperature range of 120°C to 240°C, and visual observation is done. The physical condition of polystyrene as depicted in figure 3.2 shows that at 120°C there is no significant change in the physical appearance of the pellet. With increasing temperature at 180°C polystyrene is above its glass transition temperature but still, surface forces were not dominant enough to minimize themselves and acquire a spherical shape. At 240°C polymer appears to be overheated and acquires a yellowish-red texture which is brittle. However, it is semispherical in shape and can show magnification and resolution but is not at all suitable for the proper lensing application. Polystyrene pellets over 210°C start to degrade and give yellow color lenses. While below 195°C polymer pellets do not acquire a hemispherical shape, and instead, show an elliptical profile. Thus a temperature range of 200-210°C was found to be a suitable/optimized temperature range, where the polymer pellet acquires an optically transparent semispherical shape. Lenses fabricated at 210°C were most suitable for lensing applications.

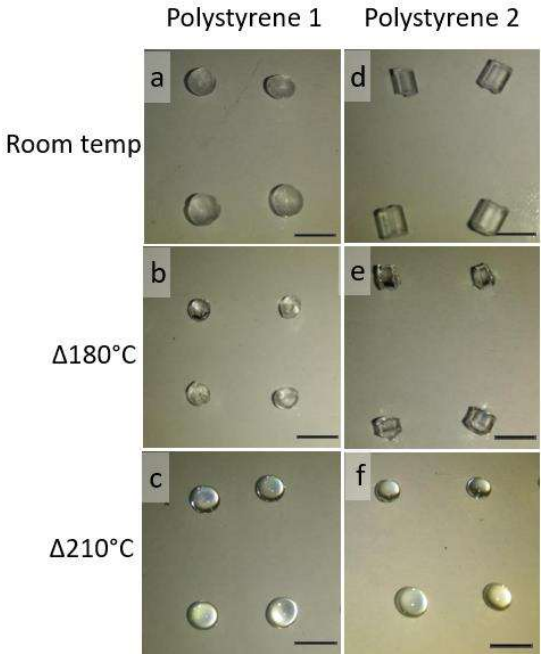

Figure 3.2 Pellets of Polystyrene of two different molecular weights at different temperatures. (a)(b)(c) Shows polystyrene 1 (of 192K molecular weight) heated at 120°C, 180°C, and 210°C for 3 hours. (d)(e)(f) is polystyrene 2 under similar parameters. It can be seen that transparency increases significantly after the thermal reflow process when the polymer is heated significantly over its glass transition temperature. The scale bar is 5mm.

Figure 3.2 shows the shape and size variation of two different molecular weight polystyrene polymers with increasing temperatures. It can be seen that, when the equilibrium condition is achieved, the curvature and contact angle of the melted pellets (further notified as lenses) is dependent on the molecular weight of the polymer but almost independent of the temperature. Since there is a narrow temperature range where pellets get the proper shape of lenses, there is negligible variation in surface tension due to temperature thus any significant variation in equilibrium shape and size is not observed. While increasing the temperature, curvature and contact angle insignificantly reduce, and by increasing the molecular weight curvature and contact angle increase. This

is as per presumption considering the free volume concept, there is negligible change in density with temperature for the polymer of a given molecular weight. Since the two polymers used in the experiment, have a significant difference in molecular weight and hence density, Observations made above are supported by WLF equation[23] which can be expressed as:

$$Log\ a_T = C_1(T - T_r)/(C_2 + T - T_r)$$

Where a_T is shift factor defined as:

$$a_T = \mu T_r \rho_r / \mu_r T \rho$$

Here C_1 and C_2 are constants, T, μ, and ρ Absolute temperature, absolute viscosity, and density of the polymer. r subscript shows properties at a reference state. Thus by increasing viscosity with molecular weight, the equilibrium curvature of the lens can be increased. The equilibrium shape of the lens depends upon the spreading function of polymer over a substrate which is defined as follows:

$$S = \gamma_{sg} - (\gamma_{sl} - \gamma_{gl})$$

Where γ_{sg}, γ_{sl}, and γ_{lg} are the surface energy of solid/gas, solid-liquid, and liquid gas interphase respectively. Since for the glass substrate, polystyrene, and air interface, spread function S < 0, we get curved lens shape polymer droplet after thermal reflow. Moreover, young's equation provides the equilibrium shape of the lenses with contact angle θ as

$$\gamma_{sg} = \gamma_{sl} + \gamma_{gl} Cos\theta$$

Also, the time required to achieve the semispherical shape, at a constant temperature, is more for the high molecular weight polymer, due to increasing entanglement with the increasing molecular weight. Another important parameter in lens fabrication is the mass

of the polymer pellet. Once the polymer is above its glass transition temperature for more than 2 hours the polymer starts to flow and acquires a curved shape, the capillary length which is the ratio of surface energy to gravity forces on the droplet determines the curvature of the droplet. For larger pellets, the gravity effect is significantly high and flattens the lens. When a pellet of smaller mass is melted, the surface force dominates the gravitational impact on the droplet and tends to become more circular giving higher curvature and lower focal length. A direct relation between the focal length and mass of the lens is established in further discussion. Since increasing temperature to more than 230°C changes the polymer property adversely, and heating for an extended time (more than 3 hours) does not make any significant difference in curvature and contact angle, effective variation in curvature and contact angle can be done through molecular weight and size of the lens only.

3.4.2 Simulation Diagram for Spot Diagram

The fabricated lens is subjected to analytical study for a spot diagram of the focus of the lens and OPD analysis using the zemax OpticStudio simulation platform. The refractive index was taken as 1.592 for the polystyrene and three wavelengths (486nm, 587nm, and 656nm) are selected to represent visible light for the simulation process and the aperture is set at 3mm. Figure 3.3a shows the spot diagram of the fabricated lens and figure 3.3b is the spot diagram of commercially available BK7 glass lenses by Edmund optics (stock no. 47-269). From the spot diagram, it can be concluded that for a wavelength higher than 520nm spot diagram is sharply focused. However lower wavelength in the blue region, the spot is mildly defocused.

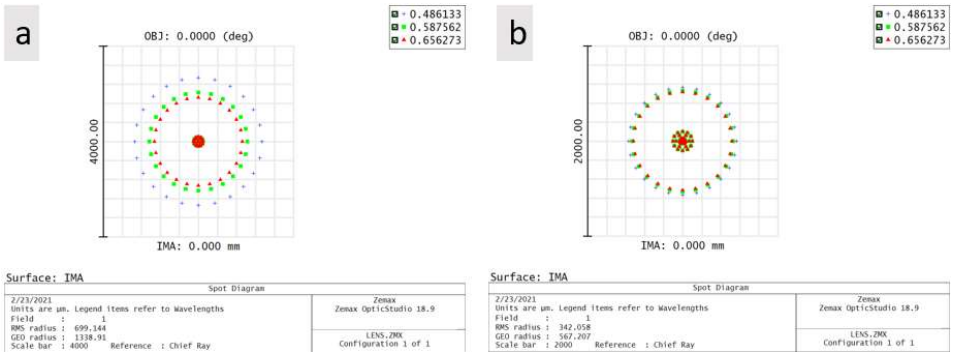

Figure 3.3 Spot diagram using Zemax OpticStudio of a) fabricated polystyrene lens and b) commercially available lens by Edmund optics.

3.4.3 Simulation Study of Lenses for Optical Path Difference

To obtain the spherical aberration in the lens optical path difference of the lenses is calculated using simulation. Figure 3.4a and b shows the OPD diagram for the fabricated lens and commercially available lens respectively. The result shows that the path difference in our fabricated lens is significantly less than in the latter. For both parameters, simulation results show that for the wavelength higher than 520nm, the effectiveness of the fabricated lens is better than the commercially available lens. It must be kept in view that the total fabrication cost of the lens in batch mode of 100 lenses is far less than 5INR, i.e. in one dollar more than 15 lenses can be fabricated, which is 600 times cheaper than the lens used for comparison.

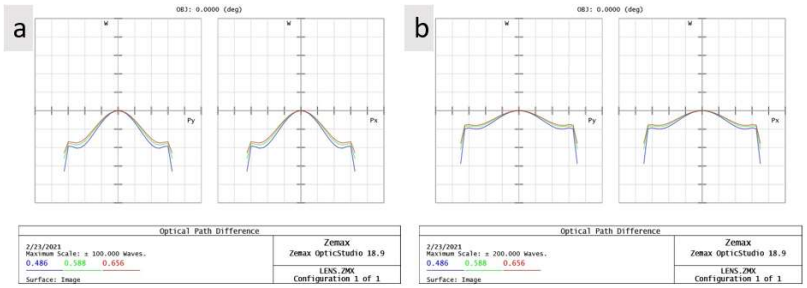

Figure 3.4 Optical path difference using Zemax OpticStudio for a) fabricated polystyrene lens and b) commercially available lens by Edmund optics.

3.4.4 Magnification and Resolution Analysis of Lenses

The magnification and resolution of lenses depending upon the focal length and numerical aperture of the lens. Figure 3.5a depicts the relation between focal length and the weight of the lens. Having the focal length estimated experimentally, the numerical aperture can be estimated using the following equation.

$$NA = n\,Sin\,\alpha = \frac{nr}{\sqrt{f^2 + r^2}}$$

Where r and f are the radius and focal length of the lens as shown in figure 3.5b, and λ is the refractive index of the medium. A lens of weight less than 30gm is having a diameter less than that of the capillary length of Polystyrene, and surface tension forces are dominant over gravity forces resulting in a low numerical aperture and high curvature and hence the short focal length. Having lower focal lengths, these lenses help to focus on very small objects placed near the integrated cellphone camera. Lenses of higher weight than 50 milligrams get more flattened due to the significant effect of gravity over surface tension forces. Such bigger lenses have large focal lengths and comparatively low numerical apertures.

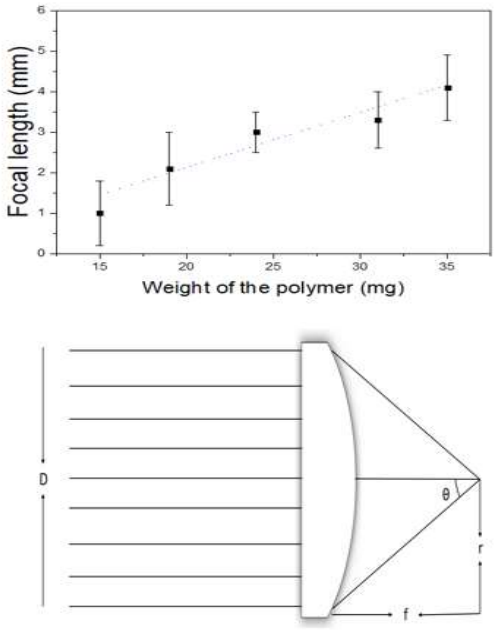

Figure 3.5 Estimated focal length plotted against the weight of the polymer shows a linear dependence. The lower focal length of the lens ensures a higher numerical aperture and higher magnification.

The magnification of lenses is demonstrated in two ways, the fabricated lens is used as an attachment to the cellphone camera, as well as placed near an object and focused through the cellphone camera. It was found that these lenses significantly reduced the focal length of the cellphone camera and were able to focus on the object from a distance of 2-3mm in both cases. (Reducing focal length in a cellphone camera is important in the cellphone-based lab on chip devices, as to image micron size objects it is important to have a significantly lower focal length than the original focal length of the camera) This lens attachment showed significant resolution and magnification when a pixel pattern of 435 PPI was imaged, as shown in figure 3.6.

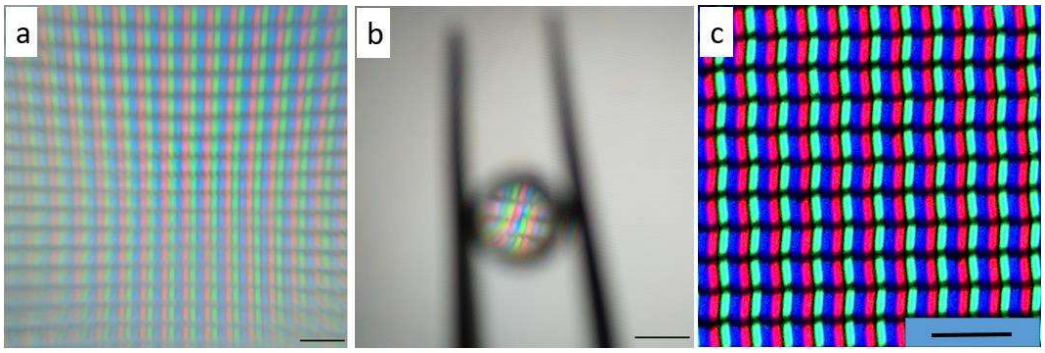

Figure 3.6 Cellphone pixel pattern observed when a) lens is attached to the integrated cellphone camera b) when the lens is kept near an object and focused through the cellphone camera. c) figure shows the pixel pattern observed from a standard microscope. The scale bar is 100µm. Scale bar is positioned corresponding to the region under best focus in a) and b).

It should be noted that when lenses were kept near object resolution and clarity of the Image were high and the field of view was less. Very high Image distortion can be seen in the case of the lens kept near an object, with a very small field of view under proper observation. When the lens was attached to the cellphone camera, the field of view was significantly high but resolution and clarity were compromised. In this case, distortion was seen only on the boundaries and a significant portion of around 1.5mm^2 was visible without distortion. The pixel color pattern used to observe consisted of red green and blue color patterns, which were very clearly distinguishable under the lens, showing lenses are almost free from chromatic aberration. Further confirmation through the simulation model by calculating optical path difference is demonstrated in the next section. However, there are other kinds of distortions in the image. The reasons for distortion in the image may be due to the non-circular rearrangement of the molten polymer pellet. Such problems can be omitted by melting the polymer in a mold and controlling the shape and size. To mount the lens over the cellphone camera, an additional transparent strip is

used above the lens, which is reducing the clarity of the image captured. It should also be noted here that since Polystyrene of higher molecular weight is having higher viscosity after melting it is having high contact angle and higher curvature, which enables the lens to have a lower focal length and higher magnification. However, it accompanies associated problems like high distortion in the image because of the high contact angle and smaller numerical aperture.

3.4.5 Observation of live cells and Tissues

To see the effectiveness, the lens is kept in the path of the microscope focus and onion peel cells are observed without any staining. When the microscope is in focus, the fabricated lens is hovered over the object to focus through the lens. A comparison of the area focused under the lens and outside the lens is made. Figure 3.7 shows the observation of an onion peel cell, focused through a lens fabricated, using the microscope. It can be seen that the area focused through the microscope shows only onion peel cells, however, the nucleus of the cells can be easily observed in the area focused under the lens. Figure 3.7b shows the onion peel cells when a 16MP (1/f = 2.1) cellphone camera is used to focus through the lens. A visual comparison shows that though the image clarity is not as high as a microscope, but cell boundaries and nucleus are easily identifiable under the lens.

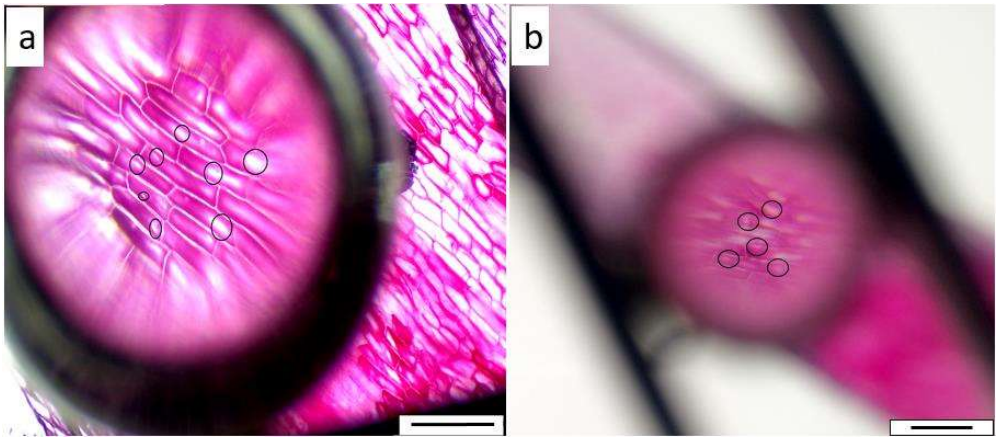

Figure 3.7 Onion peel cells observed without staining a) focused with and without the lens simultaneously through the microscope. Encircled portion shows the nucleus of the cells which is missing in the portion focused without the lens. b) focused through a lens using a cellphone camera, showing an easily identifiable nucleus of the onion peel cells. The scale bar of 100µm corresponds to the best-focused region under the lens.

In the above observation, the area focused under the lens is very small and only 9-10 cells are visible without significant distortion. To increase the field of view of the lens combination, the fabricated lens is attached to the integrated cellphone camera using transparent adhesive tape and onion peel cells are observed without staining. Figure 3.8 shows the observation of an onion peel cell, using a lens mounted on a cellphone camera. A corresponding image for comparison taken under the microscope is also provided. It can be seen that though the visual clarity is not as high as the microscope, the obtained image is good enough clear to identify the given species. Faded visibility is due to the additional adhesive tape used to mount the lens on the integrated cellphone camera.

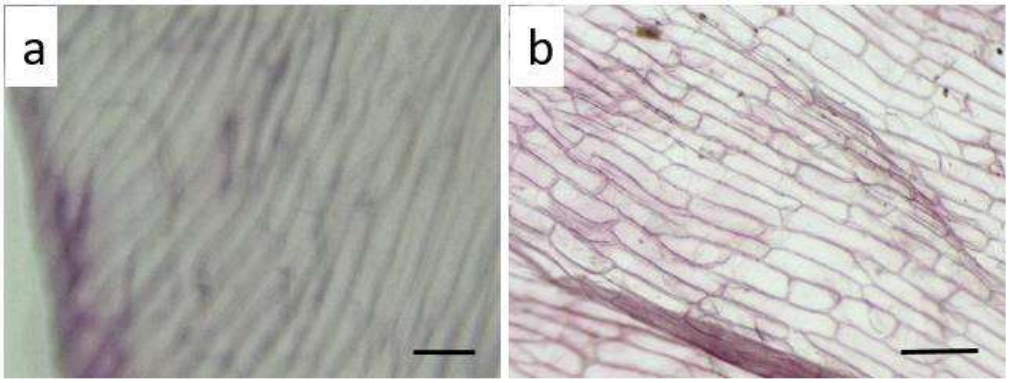

Figure 3.8 Onion peel cells observed without staining, from the a) lens attached to cellphone camera and b) from a standard microscope. Almost equal magnification is observed though visibility is compromised, which can be resolved using image processing software in the cellphone. Scale bar 100µm.

3.4.6 Experimental Observation and Future Scope

With the help of this presented work, we aim to obviate the use of the microscope, and a handheld cellphone camera along with the help of the combination of the presented lenses will be able to observe the feature size of less than 20µm. This will enable us to devise a cellphone-based lab on a chip setup that can observe feature sizes less than 20µm, leading to the observation of platelets, most of the bacteria, fungi, etc. qualitatively such devices can find applications in dermatoscopy, dentistry, agricultural fungal disease Identification. Quantification using cell tagging, multiplexing, and Image processing techniques may lead to superior applications like blood test reports, etc.

3.5 CONCLUSION

In this chapter, a lens attachment for a cellphone camera of high refractive index to facilitate better resolution using polystyrene is prepared. Polystyrene pellets are melted and using the thermal reflow method, a plano-convex lens is made on the glass substrate.

The shape and size of these lenses can be controlled using the weight of the pellets, the molecular weight of the polymer, and the temperature of the oven. The smaller the pellet used smaller the lens with high curvature, and higher magnification is obtained. Increasing molecular weight increased the curvature of the lenses and hence magnification. The temperature was having a very small impact on the final shape of the lens however the time taken to form the lens is dependent on the temperature of the oven. These lenses were used as a lens attachment to the camera as well as kept near the object and focused through the camera to observe a 435PPI pixel pattern. It was shown that when the lens was kept at the camera as an attachment it has a high field of view and low aberration in the image. While keeping these lenses near objects and focusing through the camera gives high resolution and magnification with a lower field of view. More clarity in the image is observed when the lens is kept near the object when compared to the lens attached to the cellphone camera. lenses are found to be free from chromatic aberration, as red green, and blue colors are clearly distinguishable. Different type of distortions in images and their possible solution is proposed which can be explored later. These lenses are capable to resolve less than 50μm and showed their promising application in point care biomedical imaging devices.

3.6 REFERENCES

[1]. Lee, S. A.; Yang, C. A smartphone-based chip-scale microscope using ambient illumination. Lab Chip, 2014, 14, 3056.

[2]. Granot, Y.; Ivorra, A.; Rubinsky, B. A New Concept for Medical Imaging Centered on Cellular Phone Technology. PLoS One, 2008, 3(4), 1.

[3]. World Health Organisation (WHO). Towards Access 2030: WHO Medicines and Health.

[4]. Breslauer, D. N.; Maamari, R. N.; Switz, N. A.; Lam, W. A.; Fletcher, D. A. Mobile Phone Based Clinical Microscopy for Global Health Applications. PLoS ONE, 2009, 4(7), e6320.

[5]. Seo, S.; Su, T. W.; Tseng, D. K.; Erlinger, A.; Ozcan, A. Lensfree holographic imaging for on-chip cytometry and diagnostics. Lab Chip, 2009, 9(6), 777.

[6]. Smith, Z. J.; Chu, K.; Espenson, A. R.; Rahimzadeh, M.; Gryshuk, A.; Molinaro, M.; Dwyre, D. M.; Lane, S.; Matthews, D.; Wachsmann-Hogiu, S. Cell-Phone-Based Platform for Biomedical Device Development and Education Applications. PLoS ONE, 2011, 6(3), e17150.

[7]. Pirnstill, C. W.; Coté, G. L. Malaria Diagnosis Using a Mobile Phone Polarized Microscope. Sci. Rep., 2015, 5, 13368.

[8]. Kanakasabapathy, M. K.; Sadasivam, M.; Singh, A.; Preston, C.; Thirumalaraju, P.; Venkatraman, M.; Bormann, C. l.; Draz, S. M.; Petrozza, C. J.; Shafiee, H. Rapid, Label-Free CD4 Testing Using a Smartphone Compatible Device. Sci. Transl. Med., 2017, 9, eaai7863.

[9]. Kobori, Y.; Pfanner, P.; Prins, G. S.; Niederberger, C. Novel device for male infertility screening with single-ball lens microscope and smartphone. Fertil. Steril. 2016, 106, 574.

[10]. Su, T. W.; Erlinger, A.; Tseng, D.; Ozcan, A. Compact and light-weight automated semen analysis platform using lensfree on-chip microscopy. Anal. Chem. 2010, 82, 8307.

[11]. Lee, W. I.; Shrivastava, S.; Duy, L. T.; Kim, B. Y.; Son, Y. M.; Lee, N. E. A smartphone imaging-based label-free and dual-wavelength fluorescent biosensor with high sensitivity and accuracy. Biosensors and Bioelectronics, 2017, 94, 643.

[12]. Greenbaum, A.; Zhang, Y.; Feizi, A.; Chung, P.-L.; Luo, W.; Kandukuri, R. S.; Ozcan, A. Wide-field computational imaging of pathology slides using lens-free on-chip microscopy. Sci. Transl. Med. 2014, 6(267), 175.

[13]. Tseng, D.; O. Mudanyali, C. Oztoprak, S. O. Isikman, I. Sencan, O. Yaglidere, A. Ozcan, Lens free microscopy on a cellphone. Lab Chip, 2010, 10, 1787.

[14]. Zhu, H.; Yaglidere, O.; Su, T.-W.; Tseng, D.; Ozcan, A. Cost-effective and compact wide-field fluorescent imaging on a cell-phone. Lab Chip, 2011, 11, 315.

[15]. Skandarajah, A.; Reber, C. D.; Switz, N. A.; Fletcher, D. A. Quantitative Imaging with a Mobile Phone Microscope. PloS One, 2014, 9, e96906.

[16]. Switz, N. A.; D'Ambrosio, M. V.; Fletcher, D. A. Low-Cost Mobile Phone Microscopy with a Reversed Mobile Phone Camera Lens. PloS One, 2014, 9, e95330.

[17]. Ephraim, R. K. D.; Duah, E.; Cybulski, S. J.; Prakash, M.; D'Ambrosio, M. V.; Fletcher, A. D.; Keiser, J.; Andrews, R. J.; Bogoch, I. I. Diagnosis of Schistosoma Haematobium Infection with a Mobile Phone Mounted Foldscope and Reversed-Lens Cellscope in Ghana. Am. J. Trop. Med. Hyg. 2015, 92, 1253.

[18]. Coulibaly, J. T.; Ouattara, M.; D'Ambrosio, M. V.; Fletcher, A. D.; Keiser, J.; Utzinger, J.; N'Goran, K. E.; Andrews, R. J.; Bogoch, I. I. Accuracy of Mobile Phone and Handheld Light Microscopy for The Diagnosis of Schistosomiasis and Intestinal Protozoa Infection in CoteD'Ivoire. PLoS Negl. Trop. Dis. 2016, 10, e0004768.

[19]. Cybulski, J. S.; Clements, J.; Prakash, M. Origami-Based Paper Microscope. PLoS one, 2014, 9, e98781.

[20]. Roy, A. C.; Yadav, M.; Peter, A. E.; Khanna, A.; Ghatak, A. Generation of Aspherical Optical Lenses via Arrested Spreading and Pinching of a Cross-linkable Liquid. Langmuir, 2016, 32, 5356.

[21]. Roy, A. C.; Ghatak, A. Optofluidic Lenses: Design of an Adaptable Optofluidic Aspherical Lens by Using the Elastocapillary Effect. Adv. Opt. Mater. 2014, 9, 873.

[22]. Roy, A. C.; Ghatak, A. Design of an Adaptable Optofluidic Aspherical Lens by Using the Elastocapillary Effect. Adv. Opt. Mater., 2014, 2, 874.

[23]. Wang, J.; Porter, R. S. On the viscosity-temperature behavior of polymer melts. Rheol. Acta. 1995, 34, 496.